2167-2

Advanced School on Direct and Inverse Problems of Seismology

27 September - 9 October, 2010

Surface Wave Analysis and Phenomenology

A.L. Levshin

University of Colorado
Boulder
USA

A. L. Levshin

University of Colorado, Boulder, U.S.A.

Surface Wave Analysis and Phenomenology

1. Surface Wave Analysis

The surface wave analysis scheme developed by the Center for Imaging the Earth's Interior at University of Colorado, Boulder is designed to measure surface wave characteristics discussed at my previous lecture: phase and group velocities, polarization, amplitude spectrum, and to extract 'cleaned' wanted signals.

The measurements themselves are preceded by several preprocessing procedures which are worthwhile to mention.

1.1 Preprocessing

Data obtained from different data centers around the world are usually presented as SEED volumes (Standard for the Earthquake Data Exchange, 1993). Preprocessing includes:

1) reformatting, by converting data from SEED volumes to the CSS v 3.0 relational database (Anderson *et al.*., 1993; Quinlan, 1994). The important advantage of this database in comparison with the often used SAC is the separation of seismic waveforms from the information related to the recording stations and channels and seismic events. This allows to correct or update seismic information without dealing with records themselves. Records of all stations for a given event are combined into one event volume;

2) editing, i.e. removal of isolated glitches and zero-line shifts;

3) rejection of all defective records containing unrepairable glitches, gaps or clipping;

4) decimation of broadband or intermediate-band channel traces to the sampling rate 1 Hz using decimating filters;

4) transformation of horizontal components into radial and transverse components according to the great circle backazimuth to the epicenter.

1.2 Frequency-Time Analysis

Our aim is to extract the signals we desire, related to nearly directly arriving waves that can be interpreted deterministically, from the potentially interfering multipathings and coda that are essentially stochastic in nature. Usually only direct wave trains of fundamental Rayleigh and Love modes are considered as desired signals. Still, in the next lecture I will show the analysis of crustal overtones. Unwanted signals, in particular surface wave coda, overtones, and body waves are greatly reduced in the filtered seismogram on which measurements are obtained.
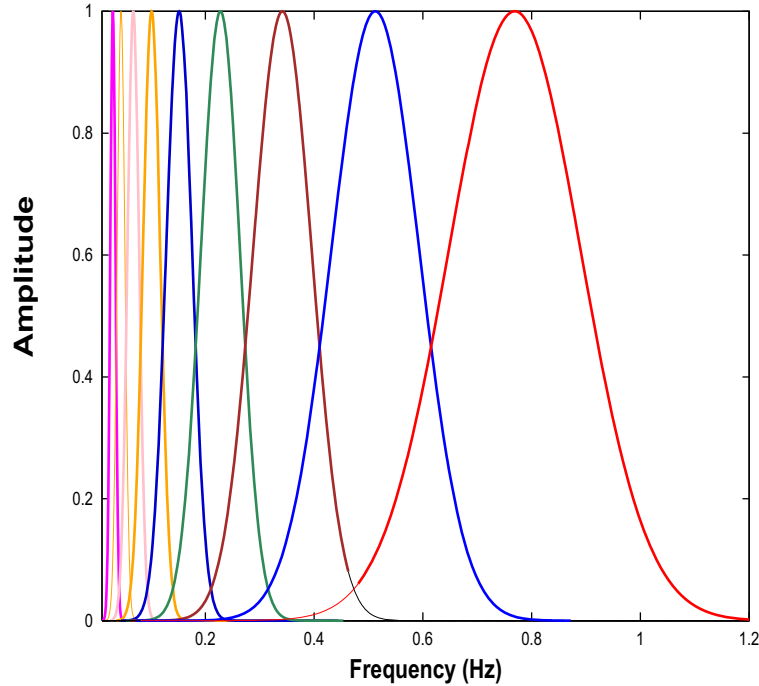
Figure 1. A comb of Gaussian frequency domain filters with constant relative bandwidth used in FTAN.

The basic characteristics of the current measurement procedure is based on a long history of development of surface wave analysis (e.g., Dziewonski *et al.* 1969, 1972; Levshin *et al.*, 1972, 1992, 1994; Levshin *et al.*, 1989; Cara, 1973; Russell *et al.*, 1988). The recent innovation is that code has been developed which allows measurements to be made rapidly on relatively large volumes of data from heterogeneous networks and a variety of source regions. The innovations have required the development of rational parametric and waveform database structures and the development of relatively rapid graphical routines for human interaction with the data (Ritzwoller *et al.*, 1995; Ritzwoller & Levshin, 1998). The general form of the measurement procedure is as follows. Group velocity - period diagrams for the vertical, radial, and transverse components are constructed using a computer-simulated system of narrow-band Gaussian filters (Figure 1).

An analyst manually traces the apparent group velocity curve for the Rayleigh wave (on the vertical and radial components) and the Love wave (on the transverse component). Time-variable filters are applied around the selected curve to separate the desired signal from the 'noise'. This results in filtered group velocity - period diagrams for which contamination from interfering signals should be reduced. Group velocity, phase velocity, amplitude, and (optionally) polarization measurements are automatically obtained on the filtered images. Measurements are graded by the analyst according to the quality of a desired signal using the 5-grade scale. All waveform and parametric data as well as surface wave measurements are stored in the CSS

2

v. 3.0 relational database which was significantly extended to accommodate this information.

An unfortunate, but currently still necessary, characteristic of this procedure, is that it depends crucially on direct human interaction with potentially large volumes of seismic waveform data. The success of this method is based on the analyst accurately identifying the main dispersion ridge of the fundamental modes, separating the 'direct arrival' from surface wave coda at periods below about 30 seconds, inspecting interpolation near spectral holes, and truncating the measurements appropriately at long periods as the signals weaken. This interaction limits the speed with which the method can be applied, and, therefore, the volume of data that can be processed. Figures 2 and 3 display this procedure.

1.3 Measurements on a Continental Scale

Due to the high average efficiency of surface wave propagation across continents, surface wave measurements can be made at periods up to 100 - 150 seconds for earthquakes as small as $M_s = 5.0$ that propagate across the entire continent. Of course, measurements can be extended to longer periods for substantially larger events.

As an example, group velocity measurements for a single station (KEVO, Finland) for one event (Kuril event, 10/9/94, $M_s = 7.0$) are shown in Figure 2b for the Rayleigh wave (measured on the vertical and radial components) at periods between about 20 and 300 seconds and for the Love wave at periods between about 30 and 250 seconds. Predictions for the spherical model PREM (Dziewonski and Anderson, 1980) are shown for comparison.

A useful by-product of these analyses are 'cleaned' or 'filtered seismograms'. Figure 2c shows a comparison between the raw and filtered seismograms for a single station:event pair. Surface wave coda, overtones and body waves have been greatly diminished from the cleaned seismograms, making them an ideal target for surface wave fitting techniques during a later stage of this research.

1.4 Measurements on a Regional Scale

On a regional scale at shorter periods, smaller events ($M_s < 5.0$) can be analyzed similarly. KNET (Kirgizian Digital Network) situated in a complex tectonic setting in Central Asia and surrounded to the East, West and South by significant seismicity is a natural site to focus studies of regional scale measurements. Due to complexity of the region records of KNET stations are usually quite complicated and exhibit a great variance of wave patterns from the same event across array and from one event to other.

Figure 3b presents an example the analysis of KNET data. Seven KNET stations were operating during the passage of surface waves from an event in the Qinghai Province, China on 1/17/94 ($\Delta \approx 16$ degrees, $M_s = 4.8$). Rayleigh and Love wave group velocity measurements are shown in Figure 3b. Rayleigh wave measurements are quite similar across the array above about 20 seconds period and for Love waves above about 30 seconds period at this azimuth. Variations across the array at shorter periods result both from real differences along the various
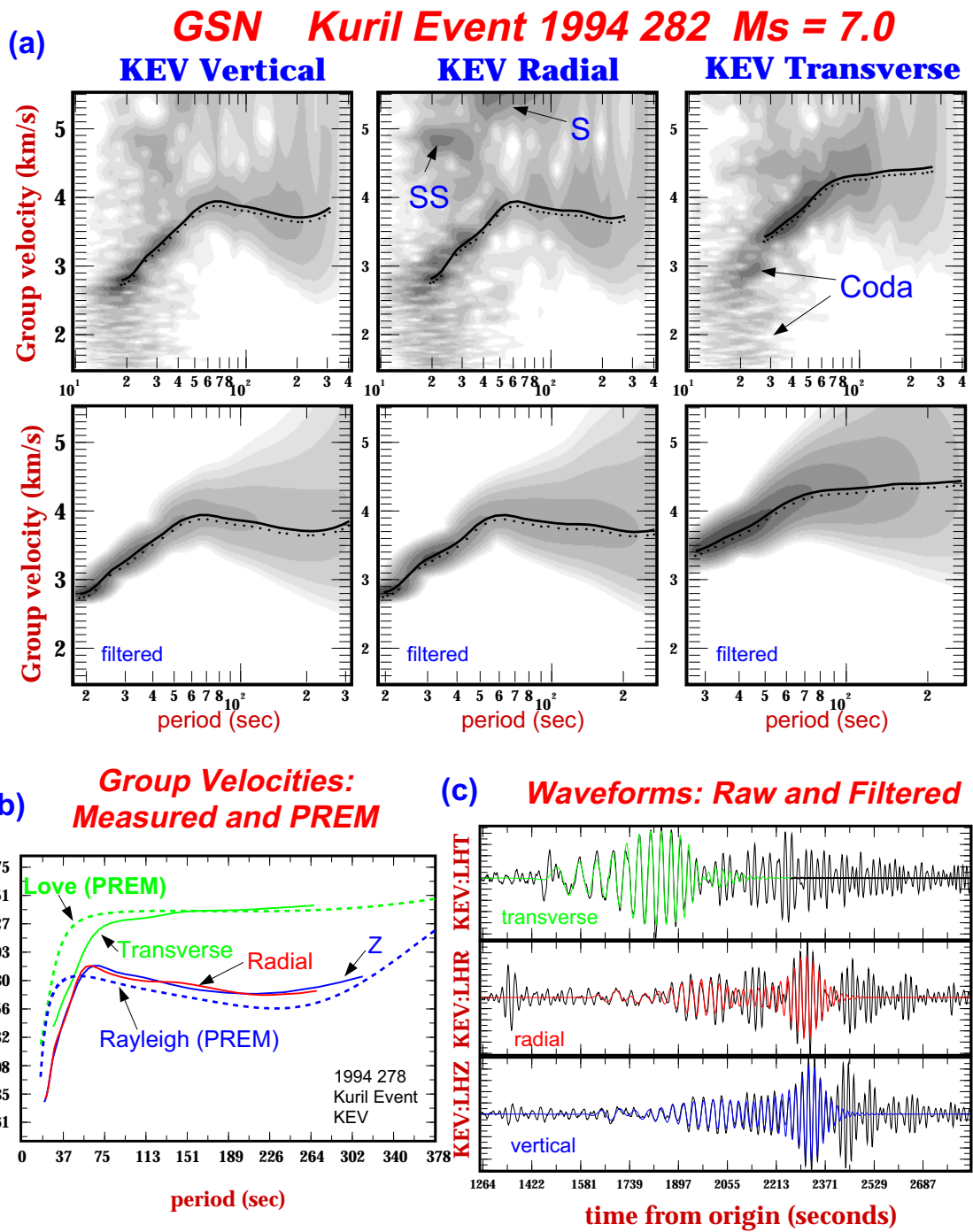
(a) GSN   Kuril Event 1994 282 Ms = 7.0

KEV Vertical   KEV Radial   KEV Transverse

(b) Group Velocities: Measured and PREM

(c) Waveforms: Raw and Filtered

Figure 2:

4

Making Regional Scale/Intermediate Period Measurements

(a) *KNET Qinghai Event 1994 27 Ms = 4.8*

(b) *Group Velocities: Rayleigh and Love*

**(c)** *Waveforms: Raw and Filtered*
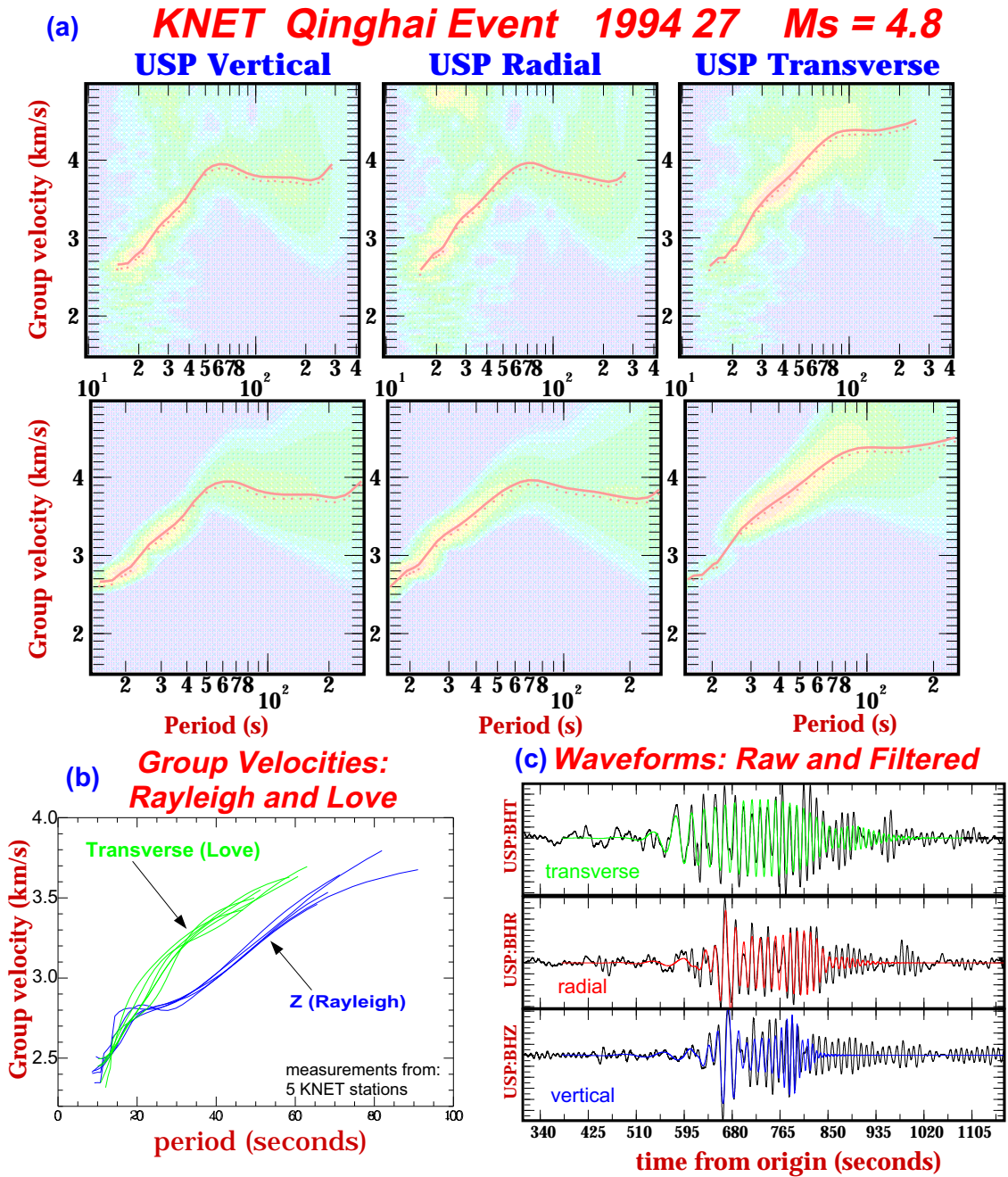
Figure 3:

wave paths near the network and also from Rayleigh - Love interference, which can be significant since the group velocities of the two wave types are similar in this period range. Cleaned and raw waveforms are presented in Figure 3c.

1.5 Measurements on a Local Scale

An interesting application of surface wave seismology is related to the off-shore seismic prospecting for oil and gas. In recent years, the technology of this industry passed through significant changes. Instead of streamers floating in the water near the surface many seismic crews use three-component bottom receivers plus hydrophones for recording seismic signals generated by air guns. The main goal is to record converted reflected PS waves which are less sensitive to the gas saturation. Presence of gas in rocks causes scattering and attenuation of P waves but produces almost no effect on S waves. Due to this seismic images obtained using PS reflections are much more focused than standard PP images. However, the serious difficulty in using PS waves is an absence of information about shear velocities near the bottom, which are needed for making static correction of PS travel times. Here is a reason to use for this purpose surface waves which are well observed if the air gun is not too far away from the bottom (10-15 m in the case of a very soft bottom, or up to 50-70 m for more hard bottom rocks).

Figure 4 provides an example of a record section from a seismic survey near Luisiana coast in Mexican Gulf. Records passed through low-pass filtering which suppresses P waves and partly suppresses PS reflection. We see several groups of slow dispersive waves which are usually called ground roll, or in this case "mud roll". FTAN diagrams for both vertical and one of horizontal components at some range are shown in Figure 5. We can distinct a fundamental (Scholte) wave at vertical component, and several higher (Rayleigh) modes at horizontal component. Some of them (like the first higher mode) are separated in a frequency-time space from others; others interfere combining in so-called guided waves: quasi-impulsive nondispersive arrivals. Our interpretation is shown in Figure 6. Resulting average cross-section obtained by Monte-Carlo inversion is shown in Figure 7. Note extremely low velocities of shear waves in upper 10 m below the bottom (40 -50 m/s), with Vp/Vs ratio of the order of 30! This demonstrates how important could be statical corrections for reconciling PP and PS images. As three-component observations become also common on land, applications of surface waves for these purposes may become more and more important.
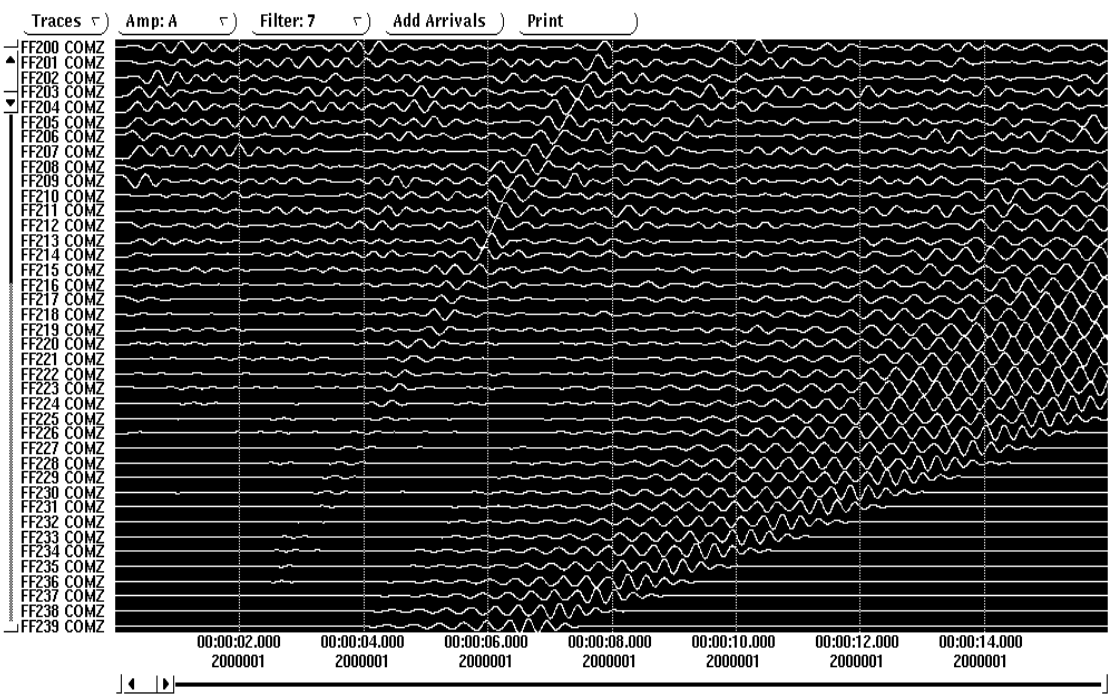
Horizontal Component
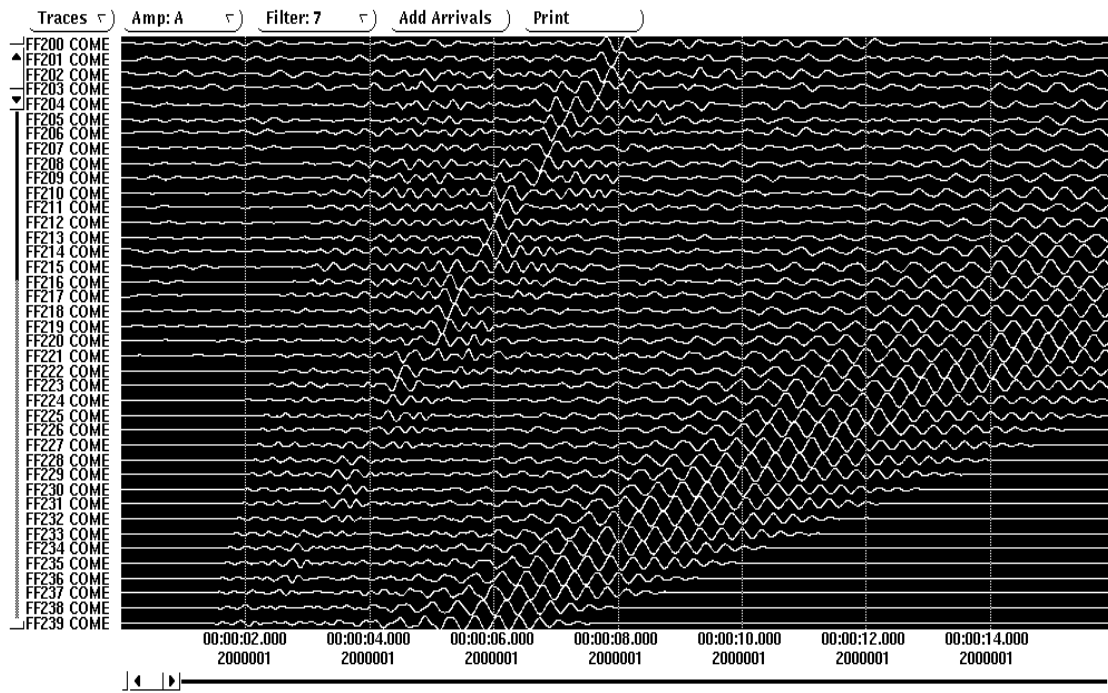
Vertical Component

Figure 4. Sea-bottom records filtered by a low-pass filter with 3 Hz corner frequency.
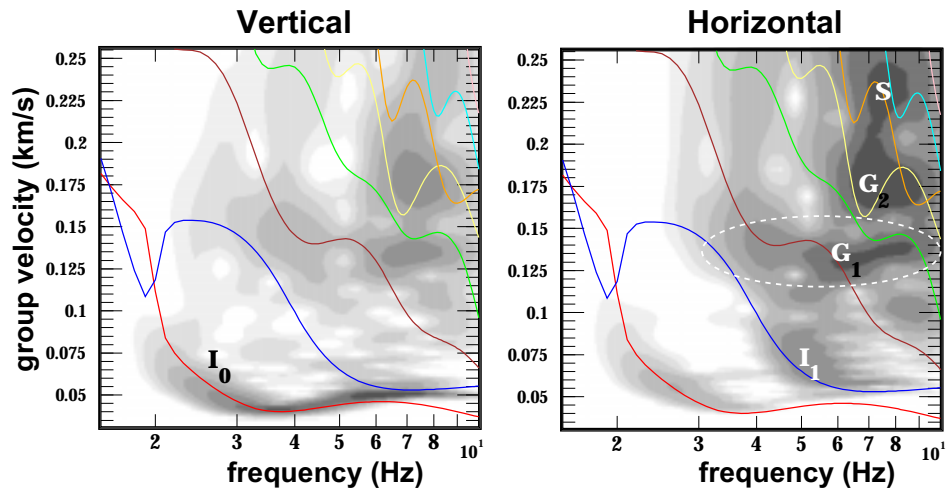
Figure 5. FTAN diagrams for two sea-bottom records.

2. Surface Wave Phenomenology

In this part of the lecture I would like to demonstrate some phenomena which are often observed during surface wave data processing.

2.1. Higher modes

First of all I would like to show an example of FTAN analysis of a real multimode record. Figure 8a demonstrates the record of the earthquake on 4 August 1998 at Iran-Turkmenistan border, at the depth 33 km. Its magnitudes are: mb=5.1, Ms=4.9. The record is made at the station Ala-Archa (AAK) near the capital of Kirgizia in Central Asia. Epicentral distance is 1560 km, the path is across Kopet-Dag mountains, Turan and Kazakh plates. The record itself looks quite complicated but FTAN diagrams (Figure 8b) show very clearly several modes of surface waves and multiple late arrivals named here CODA. Group velocities and amplitude spectra of all detected modes measured using FTAN are shown in Figure 8c. The example of interpretation of the first higher mode Rayleigh wave data will be shown at the Lecture 3.

2.2. Continental and Oceanic paths

Significant differences in surface wave propagation along oceanic and continental paths. There are at least three reasons for this:

(1) Presense of $\sim$ 5 km of water in the ocean. Love wave as a shear wave ignores the water layer. Fundamental Rayleigh mode propagates partly in water and is significantly slowed at short periods by this low velocity layer. Higher Rayleigh modes are not sensitive to water.

(2) The Earth crust is significantly thinner in the oceans (5 - 10 km) than at continents (30-50 km) and presented mostly by basalts (i.e. higher average velocities than in a continental crust).
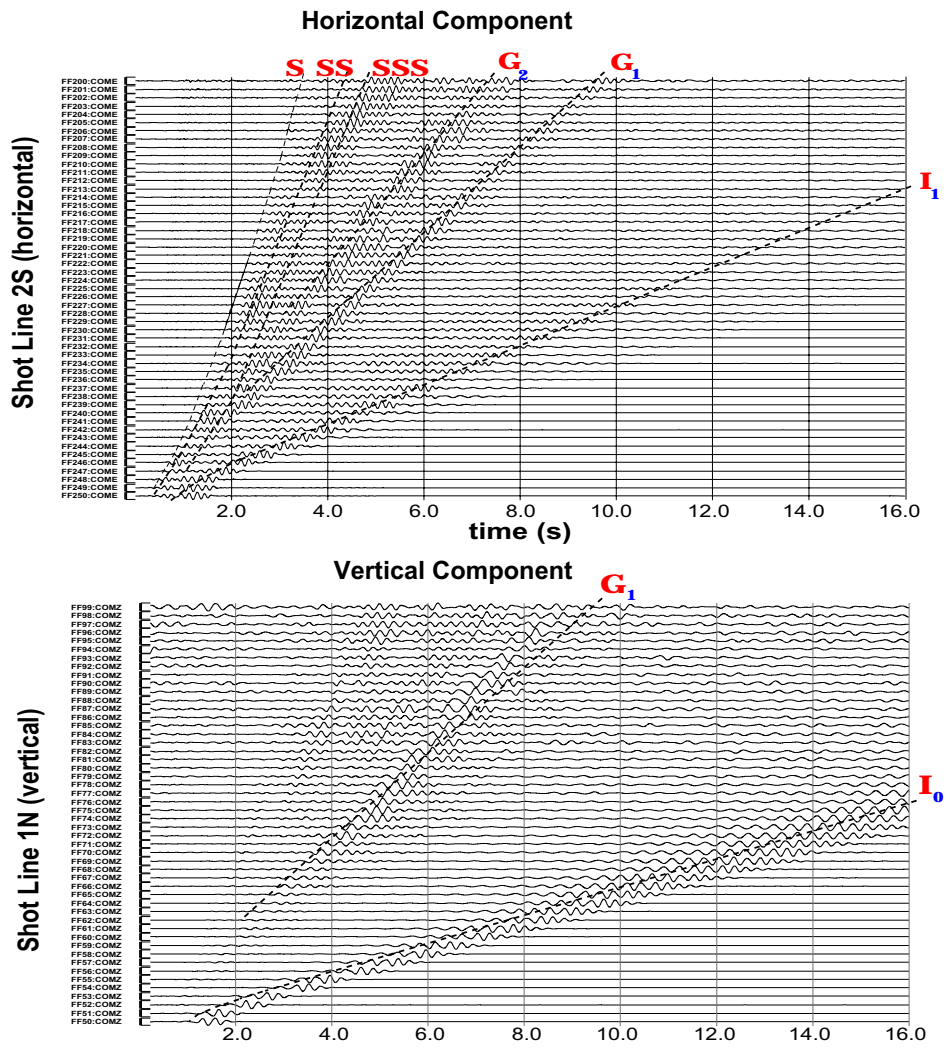
8

Horizontal Component

Figure 6. Interpretation of observed wave forms in terms of modes and waves.

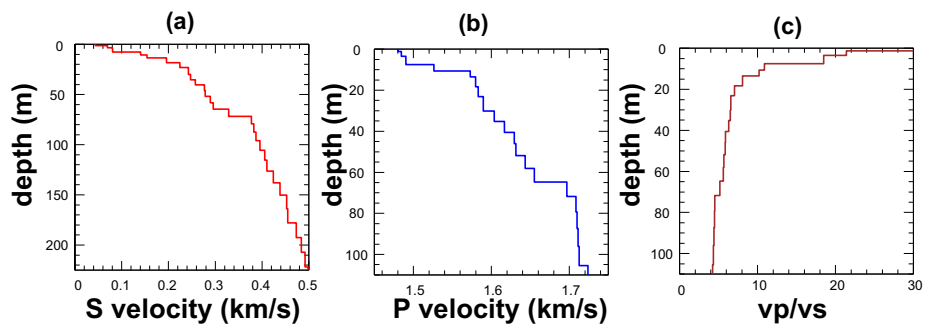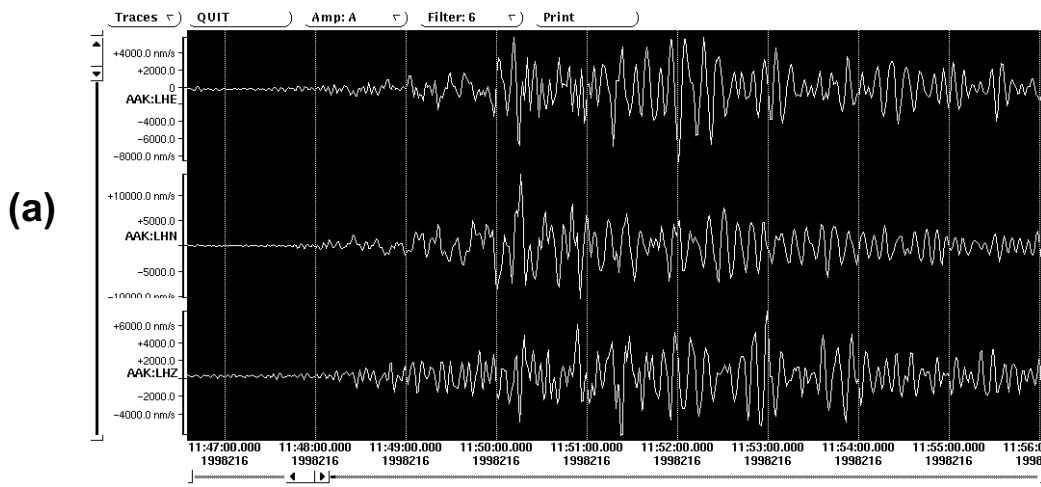**Figure 7. The average cross-section for the studied area. (a) Shear velocity; (b) Longitudinal velocity; (c) Vp/Vs ratio.**
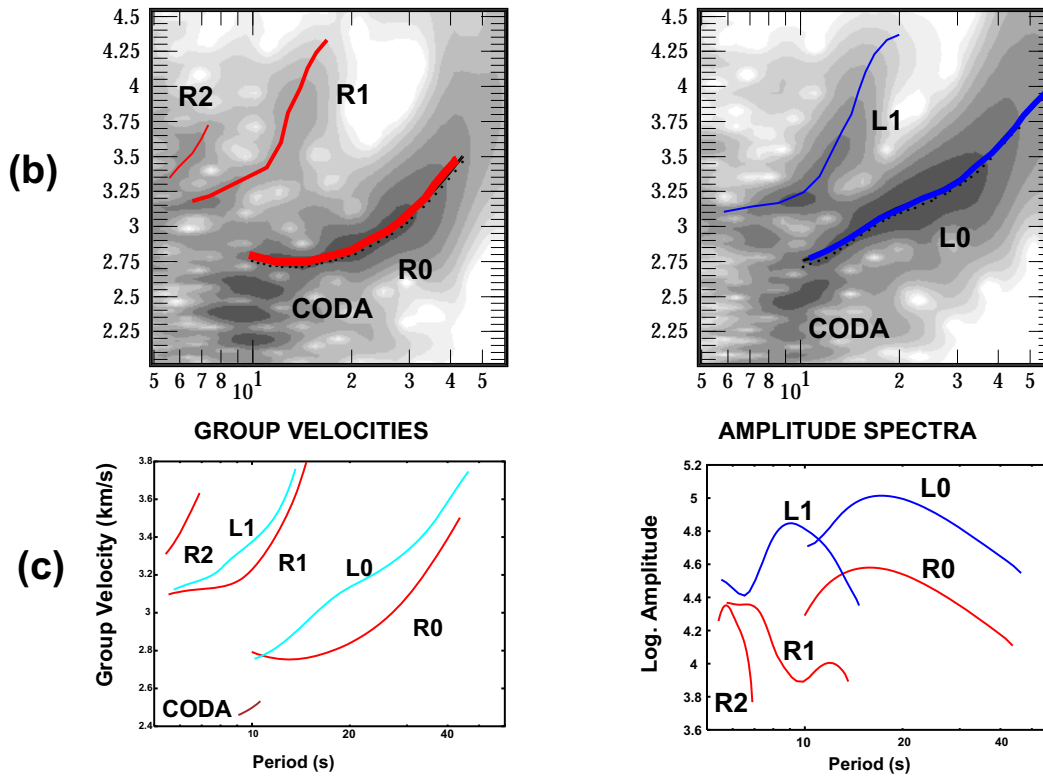
Figure 8. The earthquake at Iran-Turkmenistan border recorded at AAK (epicentral distance 1560 km): (a) records; (b) FTAN diagrams;(c) group velocities and amplitude spectra. Strong higher modes and fundamental modes of Rayleigh and Love waves are present.

(3) The oceanic lithosphere is in general more laterally homogeneous than the continental lithosphere.

Figure 9 demonstrates how different are group velocities of fundamental Rayleigh and Love waves propagating across oceans and continents. To show real data I have selected several long, purely continental and oceanic paths. Examples of Rayleigh and Love wave propagation across Eurasia are shown in Figure 10 and 11. An example of surface wave propagation across Pacific Ocean is shown in Figure 12. Note a strong scatter of short period waves (7-12 s) along the oceanic path and their practical absence along continental path. Note also some "footprints" of Love wave at vertical component, and Rayleigh wave at transverse component in contradiction to the theoretical prediction for laterally homogeneous isotropic Earth. This will be discussed later in this lecture. Very often we observe waves which paths include both continental and oceanic parts, or seas with oceanic structure of the lithosphere. The observed group velocities have intermediate values between continental and oceanic velocities. Due to the scattering effect of continental margins short-period parts of surface wave signals strongly attenuate when crossing these zones.

2.3. Path Deviations and Multipathing

As it was mentioned in the Lecture 1, the lateral inhomogeneity of the Earth is responsible for many complications in surface wave propagation. One of them, well documented in seismic literature, is the deviation of surface wave path from the shortest (great circle) paths between the source and receiver. There are two techniques for detecting such deviations. One is based on measuring travel time delays of surface wave propagating across the array or dense local network of seismic stations (e.g., Bungum and Capon, 1974). Other one is using three-component records to analyze polarization of surface waves (Lander, 1989; Paulssen et al., 1990, Levshin et al., 1992; Levshin *et al.*, 1994; Laske, 1995). Effects of relatively smooth lateral inhomogeneity will manifest themselves in deviation of the vertical plane containing Rayleigh wave particle motion from one passing through the great circle epicenter-station. Particle motion in Love waves will be orthogonal to this new plane. Figure 13 shows results of such measurements of surface wave polarization using modification of FTAN called FTPAN (Frequency-Time Polarization Analysis). These measurements were done for relatively long periods (> 60 s) to avoid Love-Rayleigh interference distorting polarization picture. Records of the Russian station (KIV) for events near S. Honshu and records of stations in Japan (INU and MAJO) for events at N. Caucasus were used to compare observed anomaly along almost reciprocal paths. Good agreement between measurements along reciprocal paths can be seen in Figure 13b. Observed Rayleigh and Love waves show significant azimuthal anomalies (up to 10° to the North) caused by increase of velocities in the upper mantle and thinning of the crust from South to North across Siberia. I should mention that most of tomographic studies do no take this effect into account. Such effects may be more severe for shorter periods (shorter wavelengths) resulting in blurring and bias at tomographic images. It is also worthwhile to mention that some anomalies
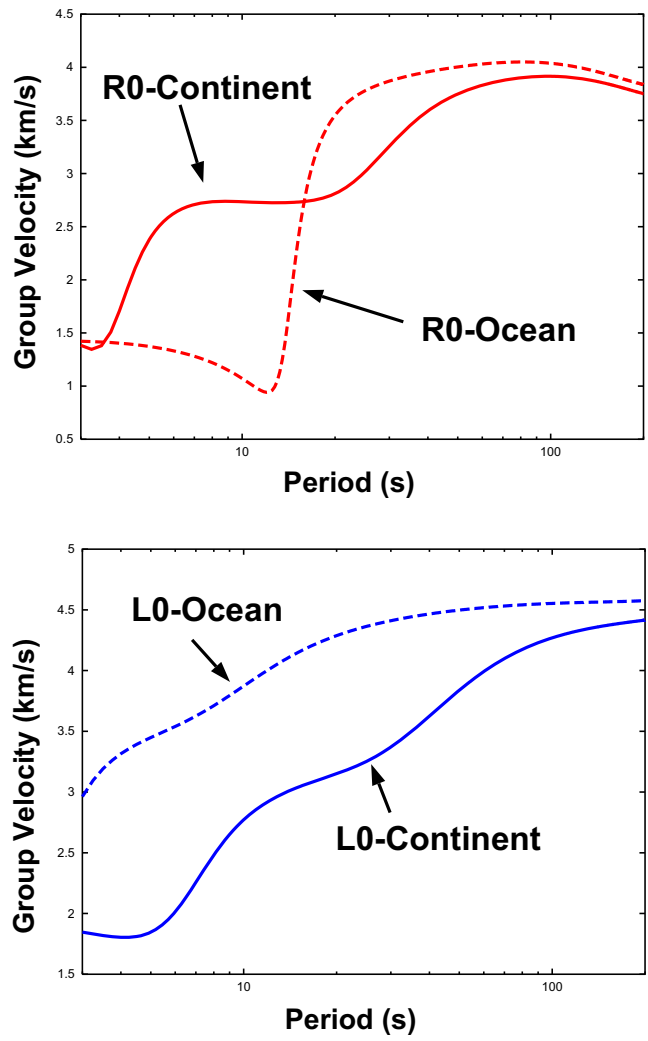
11

Figure 9. Group velocities of fundamental Rayleigh and Love waves along continental and oceanic paths.

(a)

45°N   45°N

45°E

90°E

135°E

(b)

OBN:bHZ

3.00e+04

2.00e+04

1.00e+04

0.00e+00

-1.00e+04

-2.00e+04

-3.00e+04

5 km/s

2 km/s

1000   2000   3000

time from origin (seconds)

OBN - Vertical

(c)

Group velocity (km/s)

5
4.75
4.5
4.25
4
3.75
3.5
3.25
3
2.75
2.5
2.25

R0

10^1 2 3 4 5 6 7 8 10^2 2

Period (s)

(d)

Group Velocity (km/s)

4
3.8
3.6
3.4
3.2
3
2.8
2.6

EUS

OBSERVED

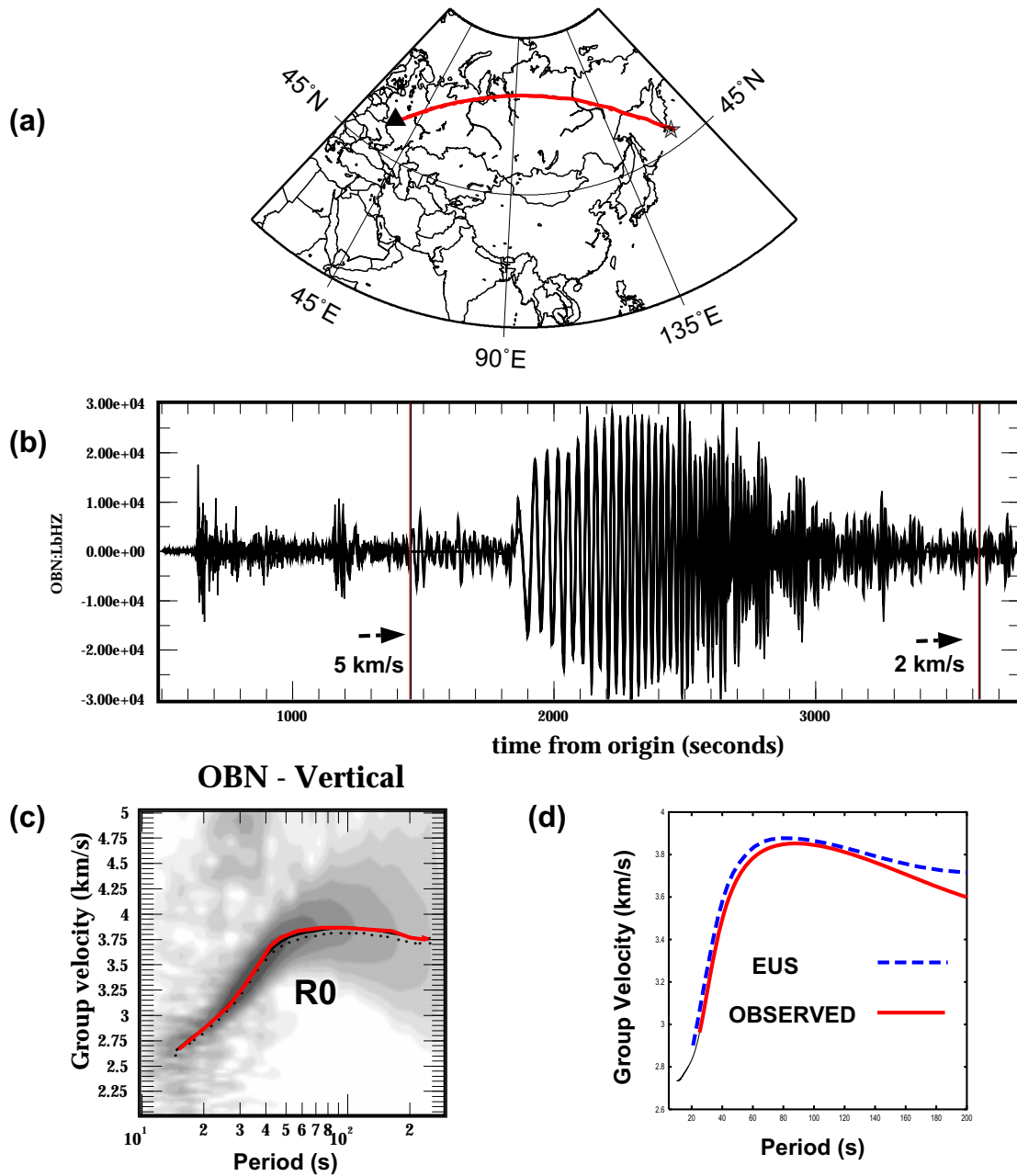20 40 60 80 100 120 140 160 180 200

Period (s)

Figure 10. Rayleigh wave propagation along a continental path: (a) Wave path across Eurasia (from N. Kuril Island to Moscow); (b) Record of the vertical component; (c) FTAN diagram; (d) observed group velocity and prediction from continental model EUS.
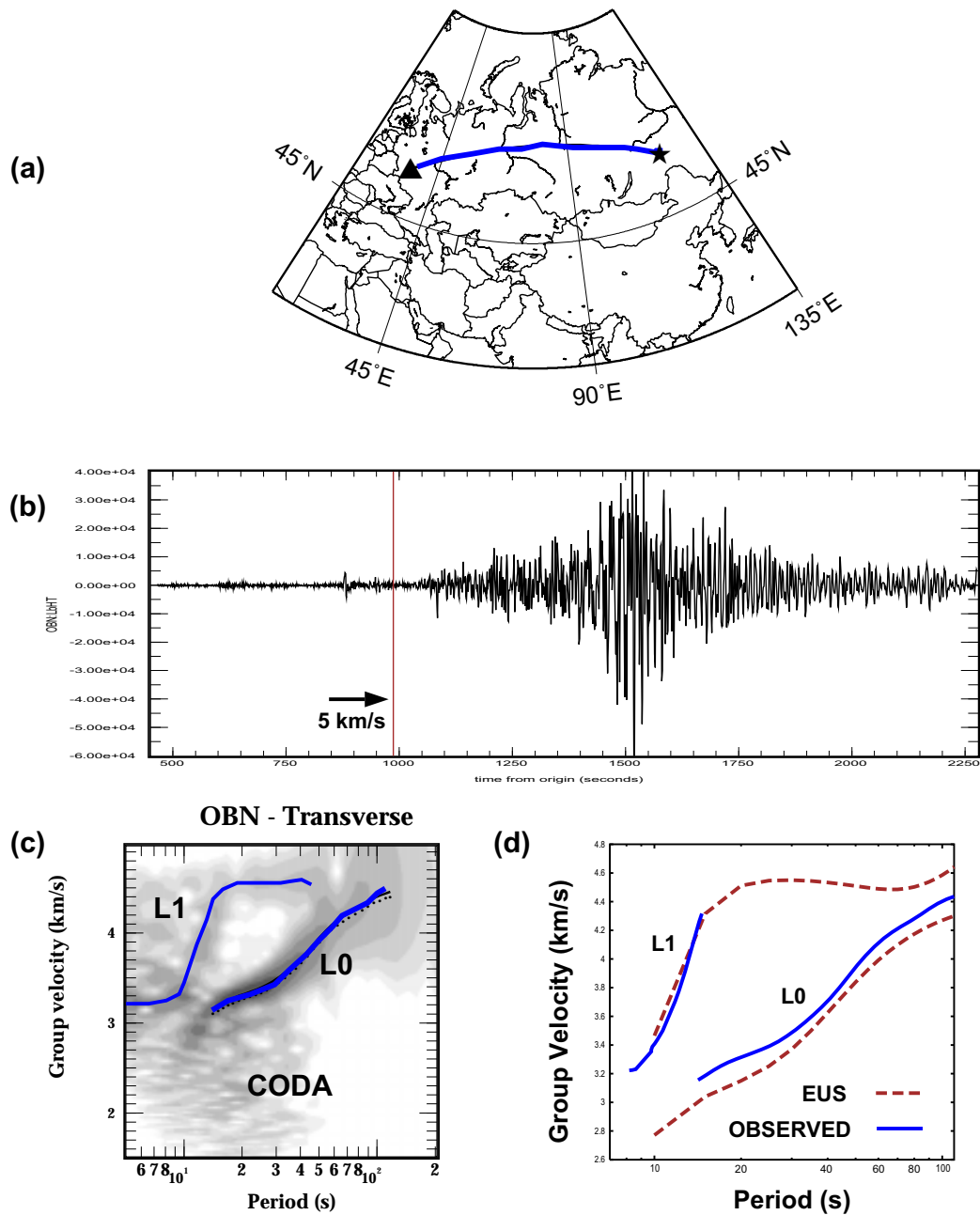
13

(a)

(b)

OBN - Transverse

(c)

(d)

Figure 11. Love wave propagation along a continental path: (a) Wave path (from E. Siberia to Moscow); (b) Record of transverse component; (c) FTAN diagram: L0 and L1 modes are seen; (d) observed group velocities and prediction from continental model EUS.
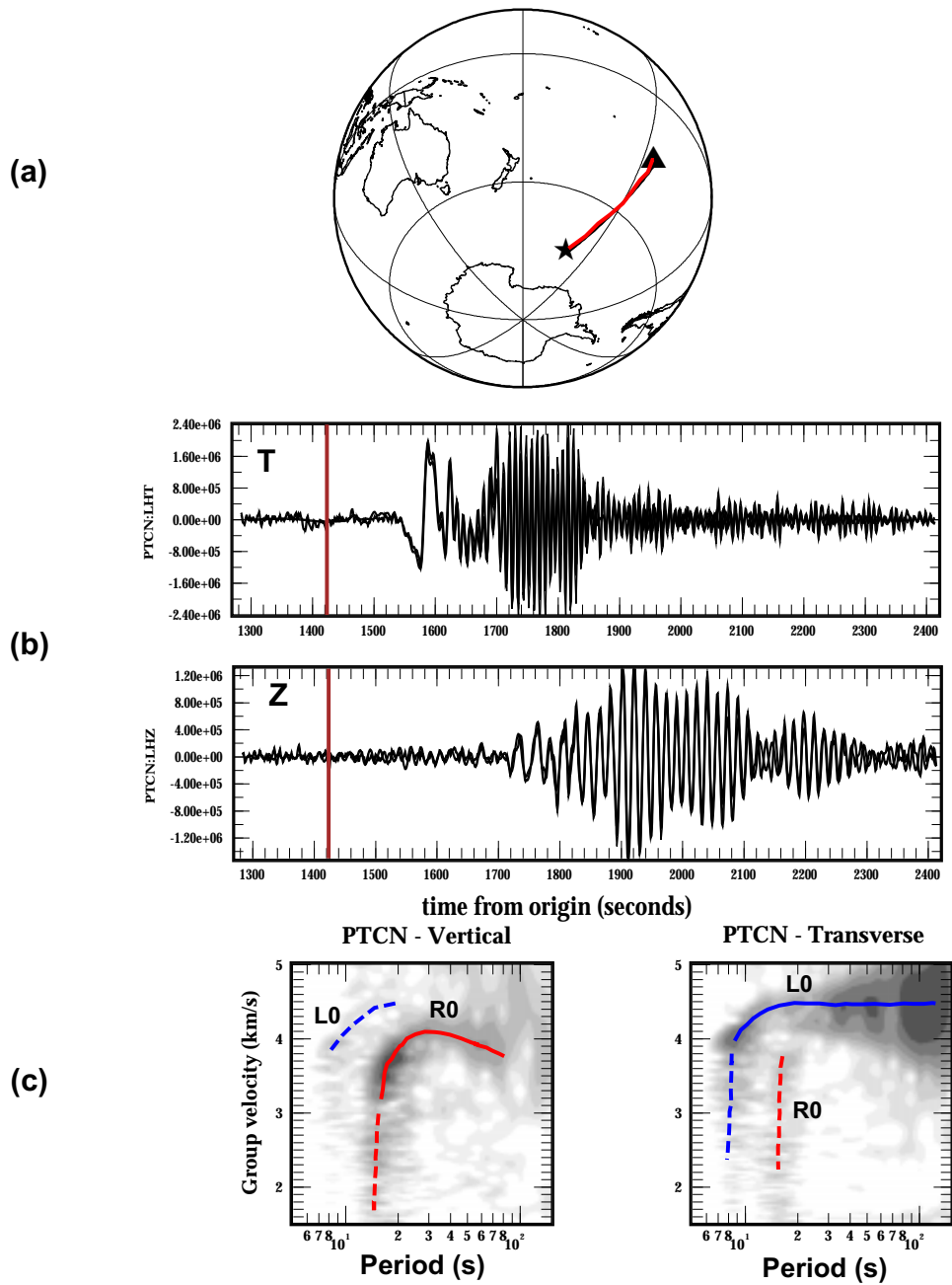
(a)

(b)

(c)

Figure 12. Surface wave propagation along an oceanic path (from Bolleny Islands near Antarctica to Pitcairn Island in Pacific Ocean, epicentral distance ~7100 km: (a) Wave path; (b) Three-component record; (c) FTAN diagrams.
Note a weak Rayleigh wave signal at the transverse (T) component and a weak Love signal at the vertical (Z) component.

of polarization may be caused by anisotropy (Crampin, 1975; Park, 1996; Levin and Park, 1998) and there are no simple rules for discrimination between two factors (lateral inhomogeneity and anisotropy) influencing surface wave polarization.

Besides deviations of the main train of surface waves from the shortest path we often observed another phenomena, namely multipathing. The part of surface wave energy splits from the main train and propagates by its own way mostly tunneled by some laterally extended low-velocity waveguide: the foredeep of some mountain range, a sedimentary basin, or the oceanic trench near the coast of a continent. It carries usually only a short-period part of the surface wave spectra and by some (yet unclear) reason consists predominantly of Love waves. Figure 14 demonstrates such a phenomenon for Love waves propagating from NW. China to the station Garm (GAR) in Tadjikistan. Latest arrival is a Love waves tunneled by Tarim Basin where thickness of sediments reaches 10-12 km. Naturally, such a wave comes much later than a direct arrival (Figure 14b), and has different angle of approach to the station (Figure 14c). Similar effects were observed in many other cases. Multipathing also may be caused by reflections of surface waves at some sharp discontinuities (boundaries of crustal blocks, rifts, deep grabens) (e.g., Levshin and Berteussen, 1979; Berteussen *et al.*, 1983), or conversion of Love waves into Rayleigh waves at sharp discontinuities.

2.5. Love in Wrong Places

This joke belongs to Prof. Jeff Park (Yale University). He discovered presence of quasi-Love waves at the vertical components of some long-period records, and explained them by effect of anisotropy (e.g., Park, 1996; Levin and Park, 1998). There are some other examples where Love waves appear at the wrong component due to other reasons:

(1) *Multipathing and path deviation* (discussed above)

(2) *Tectonic release.* Theory predicts that Love waves (as SH waves) should not be observed in a laterally homogeneous Earth if the source is a center of expansion (dilatation) or a vertical force. Nevertheless, there are excellent long-period Love waves generated by nuclear explosions. Figure 15a shows records of vertical, radial and transverse components for the nuclear explosion at Lop Nor (NW. China) obtained at the GEOSCOPE station HYB in Central India. A strong Love wave is a dominant feature of these records. Figure 15b demonstrates that surface wave group velocities observed at HYB for this explosion and for the earthquake of 11/03/1990 near Lop Nor are very similar. This implies that Love waves from the explosion are generated very close to the source and do not result from Rayleigh - Love coupling due to lateral structures along the wave path.

Observations at others stations, at quite different directions from Lop Nor, and for another set of explosions and earthquakes are similar (Levshin *et al.*, 1995; Bukchin *et al.*, 2000).

The traditional explanation of these phenomena is tectonic release provoked by the explosion in a prestressed area. There are numerous papers describing and explaining tectonic release. The interest to such phenomena is due to the fact that it makes more difficult to distinguish
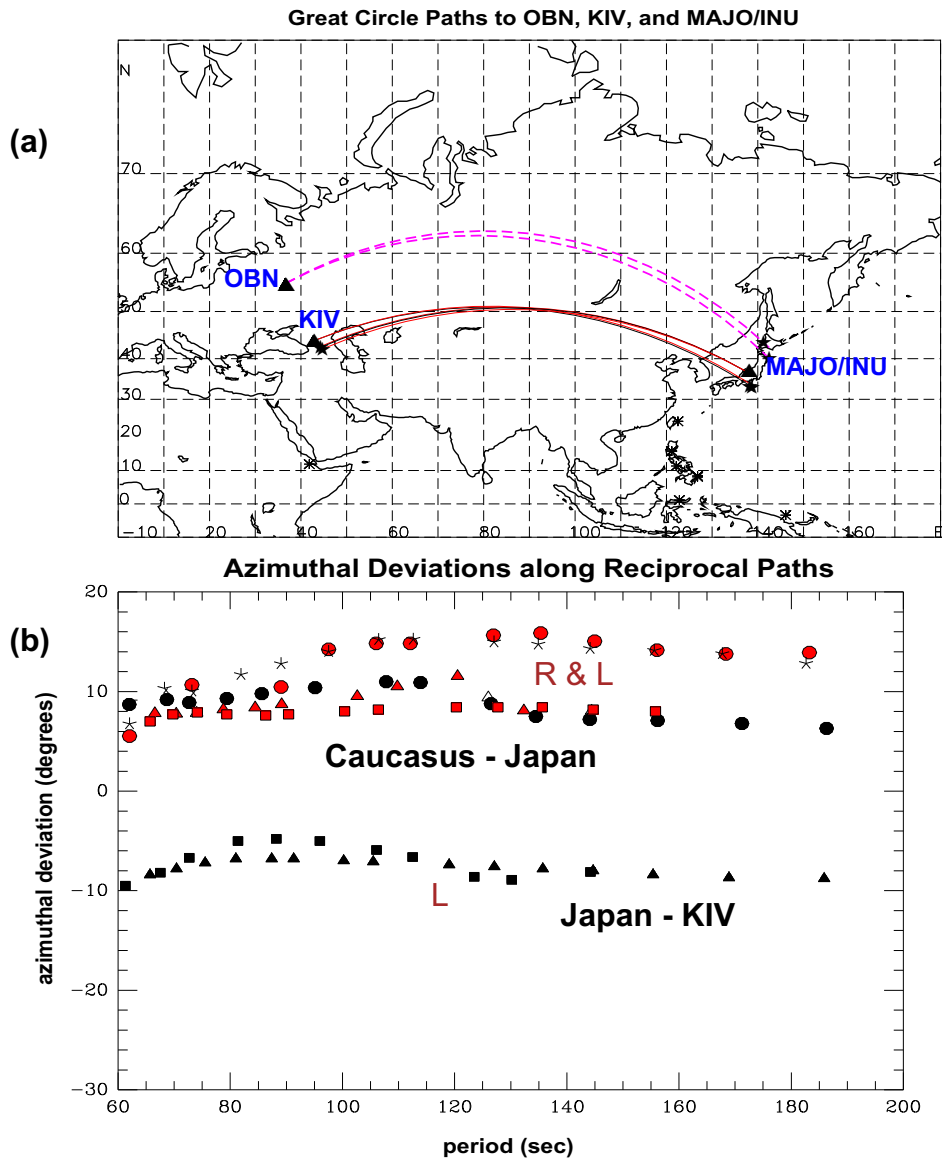
Figure 13. Azimuthal deviations of surface waves from great circle paths.
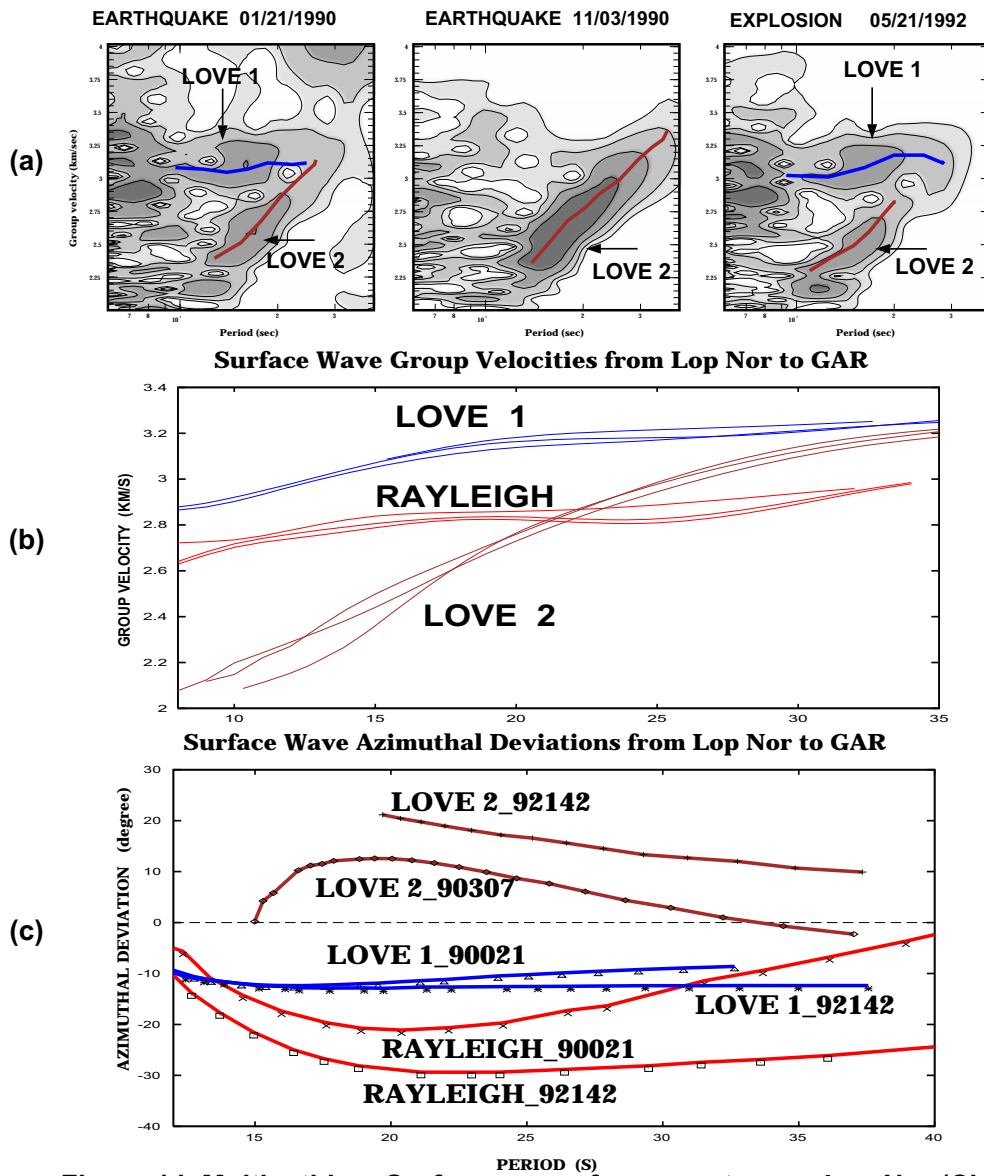
Figure 14. Multipathing. Surface waves from events near Lop Nor (China) recorded at GAR (Tadjikistan): (a) FTAN diagrams of the transverse component. (b) Group velocities of observed surface waves. (c) Azimuthal deviations of observed waves.
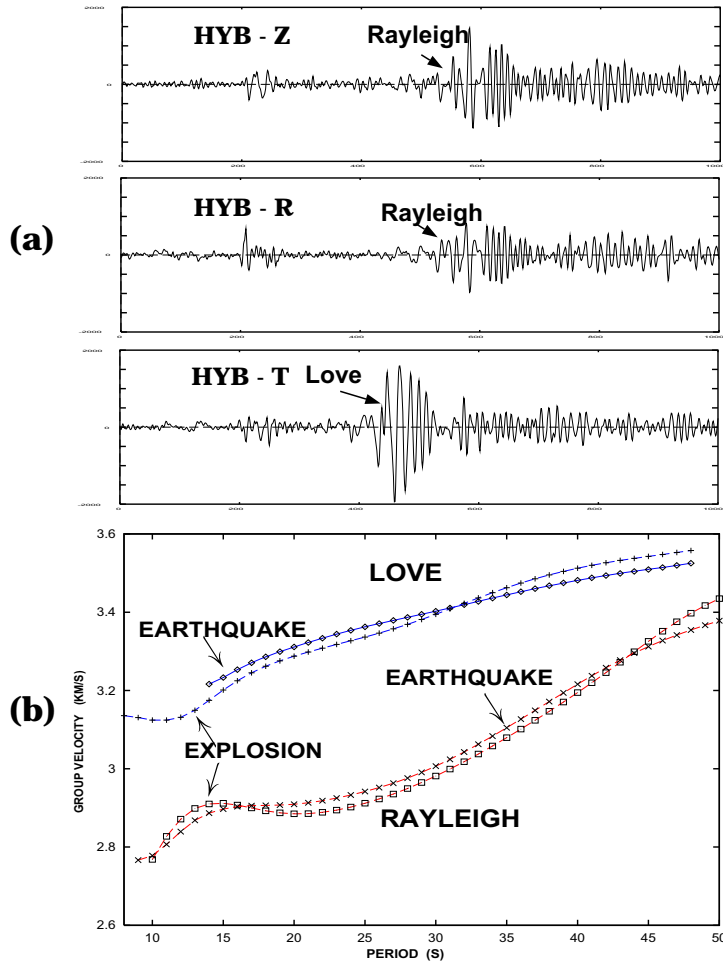
18

**Figure 15. Tectonic release from the nuclear explosion
at Lop Nor, China: (a) Love waves have the highest intensity
for the three-component seismogram of the explosion on
05/21/1992 recorded at HYB; (b) Group velocity curves for
this event and an earthquake near Lop Nor on 11/03/1990.**

between earthquakes and underground nuclear explosions using a famous $M_S : m_b$ discriminant. This discriminant is based on relative differences between body wave and surface magnitudes for explosions and earthquakes: due to the smaller size of the source zone and the shorter duration explosions are "better" generators of P waves than of surface waves. Tectonic release diminishes these differences. However, absence of isotropic component in earthquake radiation and a very small depth of the equivalent source of tectonic release from explosion may help to discriminate these events (Bukchin *et al.*, 2000).

References

Anderson, J., W. E. Farrell, K. Garcia, J. Given, and H. Swanger, Center for Seismic Studies Version 3 Database: Schema Reference Manual, CSS Technical Report C90-01, September, 1990.

Berteussen, K.-A., Levshin, A.L., and L.I. Ratnikova, 1983. Regional studies on the crust in Eurasia with surface waves recorded by the NORSAR group. In *Mathematical Models of the Structure of the Earth and the Earthquake Prediction, Comput. Seismology*, **14**, Allerton Press, NY, 106-116.

Bukchin, B.G., A.Z. Mostinsky, A.A. Egorkin, A.L. Levshin, and M.H. Ritzwoller, 2000. Isotropic and Nonisotropic Components of Earthquakes and Nuclear Explosions on the Lop Nor Test Site, China, Pure and Applied Geoph., Special volume on CTBT monitoring, Surface waves, **158**, n.8, 1497-1515.

Bungum, H., and J. Capon, 1974. Coda pattern and multipath propagation of Rayleigh waves at NORSAR, *Phys. Earth and Planet. Inter.*, **9**, 11-127.

Cara, M., 1973. Filtering of dispersed wave trains. *Geophys. J. Roy. astr. Soc.*, **33**, 65 - 80.

Crampin, S., 1975. Distinctive particle motion of surface waves as a diagnostic of anisotropic layering. *Geophys. J. R. astr. Soc.*, **40**, 177-186.

Dziewonski, A. M., S. Bloch, and M. Landisman, 1969. A technique for the analysis of transient seismic signals, *Bull. Seism. Soc. Am.*, **59**, 427 - 444, 1969.

Dziewonski, A. M., J. Mills, and S. Bloch, 1972. Residual dispersion measurements: a new method of surface wave analysis, *Bull. Seism. Soc. Am.*, **62**, 129 - 139.

Lander, A.V., 1989. Recording, identification, and measurements of surface wave parameters. In *Seismic surface waves a laterally inhomogeneous Earth*, Keilis-Borok, V.I. (Ed.),Kluwer Publ., Dordrecht, 129-182.

Laske, G., 1995. Global observation of off-great circle propagation of long period surface waves, *Geoph. J. Int.*, **123**, 245-259.

Levin, V., and J. Park, 1998. Quasi-Love phases between Tonga and Hawaii: observations, simulations and explanations, *J. Geophys. Res.*, **103**, 24321-24331.

Levshin, A. L., Pisarenko, V. F., and G. A. Pogrebinsky, 1972. On a frequency-time analysis of oscillations, *Ann. Geophys.*, **28**, 211 - 218.

Levshin, A.L., Berteussen, K.-A., 1979. Anomalous propagation of surface waves in the Barents Sea as inferred from NORSAR recordings. *Geoph.J.R. astr. Soc.*, **56**, 97-118.

Levshin A.L., Yanovskaya, T.B, Lander, A.V., Bukchin B.G., Barmin M.P., Ratnikova L.I., Its E.N. (Ed. V.I. Keilis-Borok), 1989. *Seismic surface waves a laterally inhomogeneous Earth*, Kluwer Publ., Dordrecht, 129-182.

Levshin, A. L., L. Ratnikova, and J. Berger, 1992. Peculiarities of surface wave propagation across Central Eurasia, *Bull. Seism. Soc. Am.*, **82**, 2464-2493.

Levshin, A. L., M. H. Ritzwoller, and L. I. Ratnikova, 1994. The nature and cause of polarization anomalies of surface waves crossing northern and central Eurasia. *Geophys. J. Int.*, 117, 577-590.

Levshin, A.L., and M.ʳ Ritzwoller, 1995. Characteristics of surface waves generated by events on and near the Chinese nuclear test site. *Geophys. Journal Int.*, **123**, 131 - 148.

Levshin, A.L., and M.H. Ritzwoller, 2001. Automated detection, extraction, and measurement of regional surface waves, PAGEOPH, **158**, n.8, 1531-1545.

Park, J., 1996. Surface waves in layered anisotropic structures. *Geophys. J. Int.*, **126**, 173-183.

Quinlan, D.M., 1994. Datascope: A relational database system for scientists , *Eos Trans. AGU, 75 (44)*, Fall Meet. Suppl., F431.

Paulssen, H., Levshin, A.L., Lander, A.V., Snieder, R., 1990. Time and frequency dependent polarization analysis: anomalous surface wave observations in Iberia. *Geoph.J.Int*, **103**, 483-496.

Ritzwoller, M. H., A. L. Levshin, S. S. Smith, and C. S. Lee, 1995. Making accurate continental broadband surface wave measurements. *Proceedings of the 17th Seismic Research Symposium on Monitoring and Comprehensive Ban Treaty*, Phillips Laboratory, 482-491.

Ritzwoller, M.H., and A.L. Levshin, 1998, Surface wave tomography of Eurasia: group velocities, *J. Geophys. Research*, **103**, 4839-4878.

Ritzwoller, M.H., and A.L.Levshin, 2002, Estimating shallow shear velocities with marine multi-component seismic data, Geophysics, **67** , n.6,1991-2004.

Russell, D. W., R. B. Herrmann, and H. Hwang, 1988. Application of frequency-variable filters to surface wave amplitude analysis, *Bull. Seism. Soc. Am.*, **78**, 339-354.

Standard for the exchange of earthquake data (Reference Manual, SEED Format Version 2.3), 1993. IRIS

Vernon, F., 1994. The Kyrgyz Seismic Network. *IRIS Newsletter*, **XIII**, 7-8.